

Calculation of the Temperature Distribution for Polymer Melt

G. Bognár¹, K. Marossy², E. Rozgonyi¹

¹Department of Analysis

²Department of Polymers

University of Miskolc

3515 Miskolc-Egyetemváros

HUNGARY

matvbg@uni-miskolc.hu, marossyk@gmail.com, matre@uni-miskolc.hu

Abstract: - In this paper we investigate the influence of viscous heating on capillary flows in polymer melt. The fluid properties are described by a power-law model with an exponential temperature dependence of viscosity. Solutions of the motion and energy balance equations have been obtained for nonisothermal flow in a finite length cylindrical channel. Experiments were performed to specify the rheological parameters.

Key-Words: - non-Newtonian fluid flow, viscous heating, temperature-dependent viscosity, temperature distribution

1 Introduction

In recent years, advancements in technological applications have brought a wide range of rheological fluids. The practice of non-Newtonian fluids includes extrusion of polymer fluids, colloidal and suspension solutions, molten plastics and many others. Due to the diversity of fluids in nature many models have been proposed to describe their behavior. One particular non-Newtonian model which has been widely studied is the Ostwald-deWaele power-law model.

Viscous heating can play an important role in the channel flow dynamics of fluids with a temperature-dependent viscosity such as polymers and silicate melts [4], [6]. In these fluids, the heat generated by viscous friction generates a local increase in temperature near the channel wall. The quantitative estimation of viscous heating in viscometry is a difficult matter. An overview of this subject has been given by Middleman [7]. Exact solutions are given for flows of power-law fluids, with heat generation and temperature dependent viscosity, in three situations, namely pressure flow through a circular tube, shear flow between rotating concentric cylinders and shear flow between parallel plates by Martin [8].

It is well-defined that nonisothermal flows of fluids with strong temperature dependence viscosity can lead undesirable instability in technological processes. These phenomena can be mathematically described by nonlinear governing equations [9-13].

The polymer melt that is investigated in this work is a commercial grade low density polyethylene BRALEN RB 03-23 of Slovnaft Petrochemicals [16], s.r.o., further referred to as LDPE. BRALEN RB 03-23 which is designed for production of heavy duty and shrink films of thickness 0,07 - 0,25 mm. It is well suited for blow

moulding of various containers, pipes, sheets and profiles extrusion and also for injection moulding.

In this paper we focus our investigations to the physical quantities characterizes polyethylene flow in a capillary. First, the material characterization is given to obtain the necessary data. A quantitative description of the rheological behavior of polymer melts is crucial in understanding the relation between processing and product properties. As an intermediate step between the well-defined rheometrical flows and complicated industrial processing flows, simplified, experimentally accessible, inhomogeneous flows that exhibit a combination of transient shear and elongational deformation are investigated. The detailed analysis of these flows allows the assessment of constitutive models and numerical predictions for prototype industrial flows. One of the main problems in constitutive modeling is to obtain a correct description of the transient nonlinear behavior in elongation and shear flows simultaneously. Well-known and widely used models, such as the non-Newtonian power-law model yield unsatisfactory results. The non-Newtonian viscosity depends strongly both on velocity gradient and on temperature. We shall use the power-law viscosity function. We consider an incompressible homogeneous fluid with constant density and the fluid viscosity is temperature-dependent. Although, the Arrhenius-type law of viscosity-temperature dependence relationship

$$\eta_0 = \eta_A e^{\frac{A}{RT}} \quad (1)$$

is more general and adequate to describe the polymer viscosities, for simplicity in this study we assume the Nahme-type exponential approximation

$$\eta_0 = \bar{\eta} e^{-\frac{A(T-T_0)}{RT_0^2}} \quad (2)$$

where T is temperature, A is the activation energy (a rheological factor), R is the universal gas constant and $\bar{\eta}$ is the viscosity value at the reference temperature T_0 ,

where $\bar{\eta} = \eta_A e^{\frac{A}{RT_0}}$. The Arrhenius-type law is less commonly used in the relevant literature, although this is able to fit data over a wider temperature range than the Nahme law. If we investigate the interval of temperatures for which $(T - T_0)/T_0 \ll 1$ then the Arrhenius-type relationship (1) is well approximated by (2).

The viscous heating of a finite length cylinder exposed to a steady uniform velocity non-Newtonian fluid has been analyzed. The solution determines the velocity and temperature fields of a non-Newtonian power-law model fluid in an axisymmetric cylinder. Computations were performed for an LDPE, for which the rheological parameters are determined by measurements.

Our aim is to investigate the effect of the viscous heating for temperature-dependent viscosity on the temperature distribution of the fluid.

2 Governing equations

In this paper we consider a polymeric fluid flowing axially in a capillary of radius R_0 and length l ($R_0 \ll l$). The wall temperature is assumed to be constant T_w . For the sake of simplicity, the analysis is carried out under the assumptions that the flow is one-dimensional, fluid properties, except for the viscosity factor, are constant. We postulate that

$$v_z = v_z(r), \\ v_\varphi = 0, v_r = 0, P = P(z), T = T(r),$$

where v_z is the velocity component along the flow axis, z and r , respectively, denote the axial and radial coordinates, T stands for the fluid temperature, P is the pressure. The equation of motion can be formulated as follows (see [1], [2], [6])

$$-\left(\frac{\partial P}{\partial z}\right) = \frac{1}{r} \frac{\partial}{\partial r} \left(r \eta \left(\frac{\partial v_z}{\partial r} \right) \right) \quad (3)$$

and the energy equation is

$$0 = \frac{k}{r} \frac{\partial}{\partial r} \left[r \left(\frac{\partial T}{\partial r} \right) \right] + \eta \left(\frac{\partial v_z}{\partial r} \right)^2, \quad (4)$$

where η and k , respectively, designate the viscosity and thermal conductivity of the polymer. We apply the Oswald-de Waele power-law formula for non-Newtonian viscosity ([1-6], [15]) in which the shear stress to the strain rate is described by the expression

$$\tau_{xy} = \eta \frac{\partial v_z}{\partial r},$$

where

$$\eta = \eta_0 \left| -\frac{\partial v_z}{\partial r} \right|^{n-1}. \quad (5)$$

In (5) $n > 0$ is called the power-law index. The case $n < 1$ is referred to pseudoplastic or shear-thinning fluid, the case $n > 1$ is known as dilatant or shear-thickening fluid. Most macromolecular fluids are pseudoplastic and values of n in the range of 0.15 to 0.6 are common (see [1]). The Newtonian fluid is a special case where the power-law index $n = 1$. We assume that the power-law constant n is not dependent on the temperature. In (5) constants η_0 and n are characteristic of each polymer and each polymer solution. To obtain an approximate description of non-isothermal problem the temperature dependence of η_0 is assumed by the Nahme-type law (2). In this paper we assume that the thermal conductivity k and density ρ of the fluid do not change appreciably with temperature and pressure.

The equation of continuity is satisfied identically. The equation of motion (3) and the equation of energy (4) are restated as:

$$\left(\frac{dP}{dz} \right) = \frac{1}{r} \frac{d}{dr} \left(r \bar{\eta} e^{-\frac{A(T-T_0)}{RT_0^2}} \left(-\frac{dv_z}{dr} \right)^n \right) \quad (6)$$

$$0 = \frac{k}{r} \frac{d}{dr} \left[r \left(\frac{dT}{dr} \right) \right] + \bar{\eta} e^{-\frac{A(T-T_0)}{RT_0^2}} \left(-\frac{dv_z}{dr} \right)^{n+1} \quad (7)$$

We will consider a no-slip boundary condition and axial symmetric property for the velocity. There is a constant temperature T_w at the surface $r = R_0$ for $z > 0$. The system (6)-(7) should be completed by boundary conditions:

$$v_z(R_0) = 0, T(R_0) = T_w, \\ v'_z(0) = 0, T'(0) = 0. \quad (8)$$

It is convenient to introduce dimensionless quantities

$$\theta = \frac{A}{nR} \frac{T - T_0}{T_0^2} \quad \text{and} \quad \xi = \frac{r}{R_0}.$$

Integrating (6) with respect to z from 0 to l (the total length of the capillary) we obtain

$$-\frac{dv_z}{dr} = \left(\frac{P_l - P_0}{2l\bar{\eta}} R_0 \right)^{\frac{1}{n}} e^{\theta} \left(\frac{r}{R_0} \right)^{\frac{1}{n}} \quad (9)$$

and for $v_z(r) = v(\xi)$

$$v_z(r) = -\alpha e^{\theta} \frac{n}{n+1} r^{\frac{n+1}{n}} + C_1$$

with $\alpha = \left(\frac{P_l - P_0}{2l\bar{\eta}} R_0 \right)^{\frac{1}{n}}$. Since,

$$v(\xi) = \frac{-\alpha n R_0}{n+1} e^{\theta} \xi^{\frac{n+1}{n}} + C_1,$$

and C_1 can be determined from the boundary condition

$$v(\xi = 10^{-3}) = 0 = \frac{-\alpha n R_0}{n+1} e^{\theta} + C_1$$

one can get

$$v(\xi) = \frac{\alpha n R_0}{n+1} e^{\theta} \left(\left(10^{-3} \right)^{\frac{n+1}{n}} - \xi^{\frac{n+1}{n}} \right). \quad (10)$$

Applying (9) the energy equation (7) can be rewritten

$$\frac{k}{r} \frac{dT}{dr} + k \frac{d^2T}{dr^2} + \bar{\eta} e^{\theta} \left(\frac{P_l - P_0}{2l\bar{\eta}} R \right)^{\frac{n+1}{n}} \left(\frac{r}{R} \right)^{\frac{n+1}{n}} = 0,$$

and by the dimensionless quantities

$$\frac{d^2\theta}{d\xi^2} + \frac{1}{\xi} \frac{d\theta}{d\xi} + \gamma e^{\theta} \xi^{\frac{n+1}{n}} = 0, \quad (11)$$

where

$$\gamma = \frac{A R_0^2}{k n T_0^2 R} \bar{\eta}^{-\frac{1}{n}} \left(\frac{P_l - P_0}{2l} R_0 \right)^{\frac{n+1}{n}}.$$

3 Rheological behavior of LDPE

In this section the experimental determination of the material parameters is discussed.

Flow curves were measured by a Göttfert extrusimeter 20 using a screw of 1:4 compression rate and long compression zone. The diameter of the screw is 20 mm and the L/D is 20. A round steel capillary die was used with 2.0 mm bore and 30 mm length. Inlet angle was 90°. The die is fixed in the extruder barrel. Melt temperature and melt pressure can be measured at three points along the barrel. In order to minimize the measuring errors the temperature sensor thermocouple is isolated from the barrel by a ceramic of low thermal conductivity. Only the values obtained from the sensors placed at 20D (just before the die) were used in this

study. Mass flow G was determined by weight measurement of extruded rods cut in 1 minute period.

Extrusion tests were carried out at 3 temperature setting using 160°C, 170°C and 180°C steel temperature at the die zone, respectively. Temperature of previous zones were set by 5°C lower (e.g. 150, 155 and 160°C). In consequence of internal friction heating, the measured mass temperature ϑ is always higher than the set-point of the zone heating.

Five different screw speeds ($\bar{n} = 20, 40, 60, 80,$ and 100 rpm) were applied for every temperature setting.

The measured data are given in Table 1.

\bar{n} rpm	G g/min	160 °C		170 °C		180 °C	
		P3 bar	ϑ °C	P3 bar	ϑ °C	P3 bar	ϑ °C
20	6	108	162.2	100	173.4	93	183.6
40	12	130	162.7				
40	12.2			120	173.7		
40	12.5					115	184.5
60	19	143	163.5	135	174.3	130	184.8
80	24.5	155	164.2	145	174.5	135	185.1
100	31	162	164.6				
100	31.5			155	175.3	145	185.3

Table 1.

From these measured data one can evaluate the shear rate by using the Rabinowitsch formula

$$\dot{\gamma} = \left(\frac{3n+1}{n} \right) \frac{G}{\pi r^3 \rho},$$

the shear stress

$$\tau = \frac{r \Delta p}{2l},$$

and the dynamic viscosity

$$\eta = \frac{\tau}{\dot{\gamma}}.$$

The calculated flow characteristics ($\dot{\gamma}$, τ , η) are represented in Table 2-4 for different temperature values.

$\dot{\gamma}$	$\tau_{(160)}$	$\eta_{(160)}$	$\vartheta_{(160)}$	$1000/T_{(160)}$
236.862	182304	769.7	162.2	2.29695
473.724	219440	463.2	162.7	2.29431
750.063	241384	321.8	163.5	2.29011
967.187	261640	270.5	164.2	2.28645
1223.79	273456	223.45	164.6	2.28436

Table 2. Flow characteristics at 160 °C

In Fig. 1 the measured pressure vs. extruder mass flow is shown for 160°C. The logarithm of the pressure vs. logarithm mass flow can be represented approximately by straight line (see Fig. 2) for the same temperature.

$\dot{\gamma}$	$\tau_{(170)}$	$\eta_{(170)}$	$\vartheta_{(170)}$	$1000/T_{(170)}$
236.862	168800	712.7	173.4	2.23934
481.619	202560	420.6	173.7	2.23784
750.063	227880	303.8	174.3	2.23484
967.187	244760	253.1	174.5	2.23384
1243.53	261640	210.4	175.3	2.22985

Table 3. Flow characteristics at 170 °C

$\dot{\gamma}$	$\tau_{(180)}$	$\eta_{(180)}$	$\vartheta_{(180)}$	$1000/T_{(180)}$
236.862	156984	662.8	183.6	2.18933
493.463	194120	393.4	184.5	2.18503
750.063	219440	292.6	184.8	2.18360
967.187	227880	235.6	185.1	2.18217
1243.53	244760	196.8	185.3	2.18122

Table 4. Flow characteristics at 180 °C

If a logarithmic plot of P3 versus G is gathered then the points are well approximated by a straight line (see Fig. 2) and from the slope of the line the power-law exponent n can be found:

160 °C	0.24776
170 °C	0.26555
180 °C	0.26694

It seems that n is temperature dependent. For simplicity we take it constant with the average value: $n=0.26$.

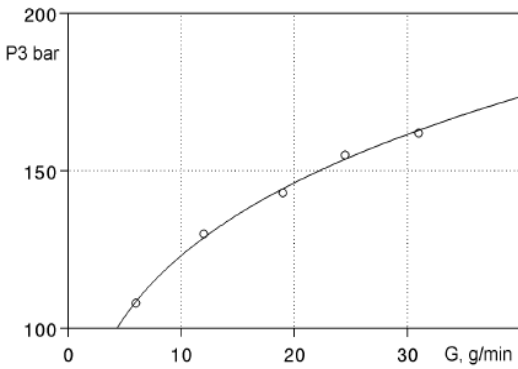


Figure 1.

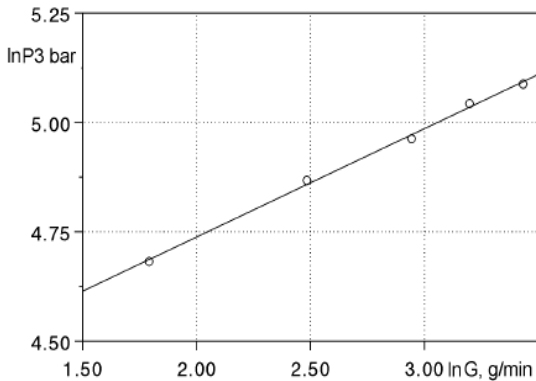


Figure 2.

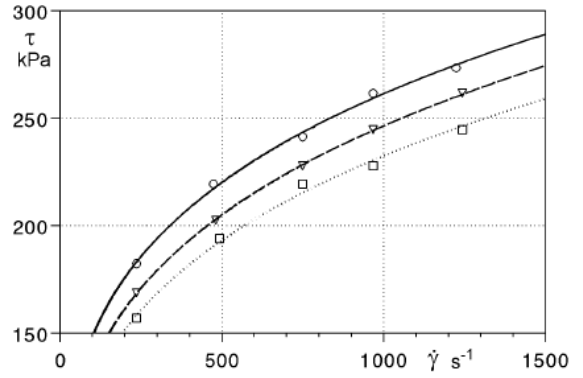


Figure 3.

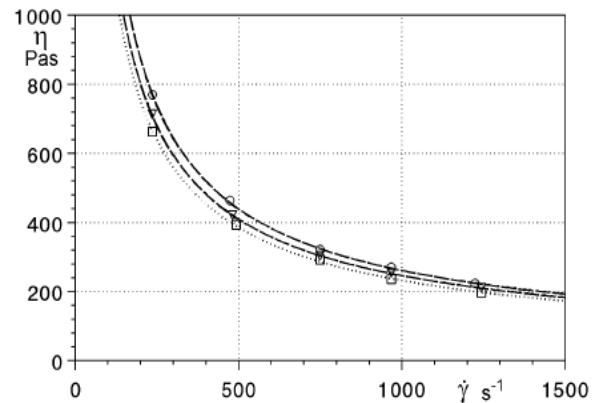


Figure 4.

On Fig. 3 the shear stress vs. shear rate is illustrated at 160°C (solid line), 170°C (dashed line) and 180°C (dotted line). The viscosity vs. shear rate is exhibited at different temperatures: 160°C (solid line), 170°C (dashed line) and 180°C (dotted line) in Fig. 4.

Points $(\dot{\gamma}, \tau)$ and $(\dot{\gamma}, \eta)$ are well approximated by power expressions. Shear stress (τ) and viscosity (η) v.s. shear rate at 160°C steel temperature are displayed in Fig. 5.

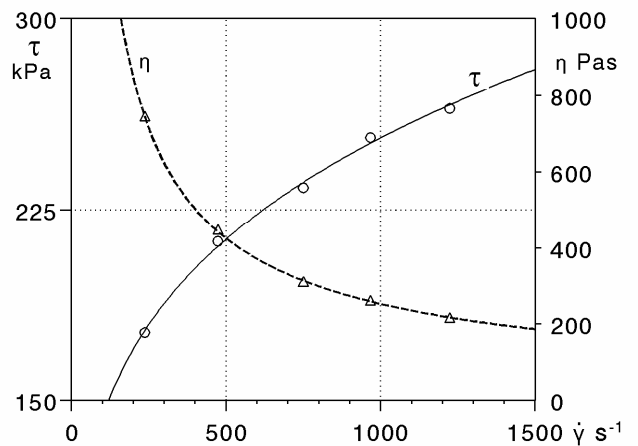


Figure 5.

The point set $(\dot{\gamma}, \eta)$ can be approximated by power functions of the form:

$$\begin{aligned} 160\text{ }^\circ\text{C} & \quad \eta = 42277 \dot{\gamma}^{-0.7524} \\ 170\text{ }^\circ\text{C} & \quad \eta = 39628 \dot{\gamma}^{-0.7354} \\ 180\text{ }^\circ\text{C} & \quad \eta = 36785 \dot{\gamma}^{-0.7331} \end{aligned}$$

The density was measured $\rho = 920\text{ g/cm}^3$. We note that $\rho = 919\text{ g/cm}^3$ is given by the Slovnaft [16]. The specific heat c_p is determined by DSC measurement for polymer melt at 160 °C

$$c_p = 2.28\text{ kJ/kg K}$$

which shows good correlation with $c_p = 2.3\text{ kJ/kg K}$ found in the literature [14].

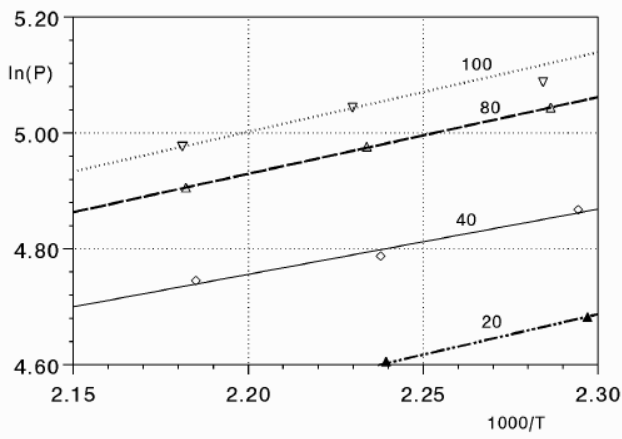


Figure 6.

In Fig. 6 $\ln(P3)$ v.s. reciprocal temperature is plotted of PE extrusion when the parameter is the screw speed (rpm). The graph is plotted using the measured mass-temperature in front of the die. Because the output (mass flow) is almost independent of the temperature, depends on the screw speed only, the pressure can be used for energy of activation calculations. The heat dependence of the viscosity is exhibited on Fig.6 is found to be suitable approximated by the Arrhenius-law (1). The linear approximations of the plots are the following:

$$\begin{aligned} \bar{n} = 20 & \quad \ln P3 = 1.4946 + 1.3880 \frac{1}{T} \text{ [kJ/mol]} \\ \bar{n} = 40 & \quad \ln P3 = 2.2800 + 1.2500 \frac{1}{T} \text{ [kJ/mol]} \\ \bar{n} = 80 & \quad \ln P3 = 2.0157 + 1.3246 \frac{1}{T} \text{ [kJ/mol]} \\ \bar{n} = 100 & \quad \ln P3 = 1.9860 + 1.3710 \frac{1}{T} \text{ [kJ/mol]} \end{aligned}$$

In the further calculations the average of the slopes 1.388 will be applied. Then one can obtain the energy of activation: $A = 11.08\text{ kJ/mol}$

4 Numerical Results

In this section we apply the previous theoretical results to the study of the temperature distribution along the capillary.

Equation (11) is solved for the dimensionless temperature θ subject to the boundary conditions

$$\theta(10^{-3}) = \frac{A}{nR} \frac{T_w - T_0}{T_0^2},$$

$$\theta'(0) = 0.$$

Calculations for the LDPE, characterized in Section 3, were carried out with following data:

$$l = 30\text{ mm},$$

$$R_0 = 1\text{ mm}.$$

The calculated temperature profiles are presented in Fig. 7 at 160°C for different screw speeds.

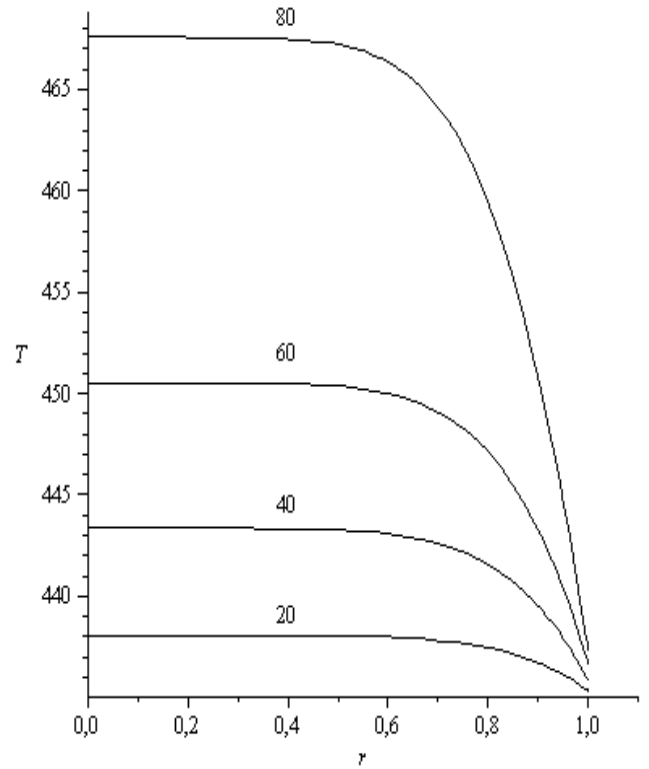


Figure 7.

At the center of the capillary the temperature increase is presented in Table 5 for 160°C, 170°C and 180 °C steel temperature and for different screw speed values. The numerical results show that even in the examined few hundred [s^{-1}] shear rate the temperature growth is remarkable. In case of heat sensible materials the heat increase can cause serious manufacturing problems.

\bar{n} [rpm]	$\Delta T(160)$ [K]	$\Delta T(170)$ [K]	$\Delta T(180)$ [K]
20	2.719	2.382	2.223
40	7.492	6.341	6.976
60	13.852	13.248	15.508
80	33.226	24.496	21.466

Table 5.

5 Conclusion

In this paper solutions are given for flows of power-law fluids with heat dependent viscosity. The results are applied for a polymer, for a commercial, general purpose grade of low density polyethylene. The rheological characterization of this material is discussed in Section 3. The assumptions are made that the capillary is sufficiently long for the attainment of a steady profile. The power-law constant n is calculated from the slope of a best fitting straight line on a logarithmic flow volumetric rate-pressure plot. The temperature growth is determined numerically at the center of the capillary for isotherm boundary condition.

List of symbols:

c_p specific heat	[J/kg K]
k heat conductivity	[W/m K]
l length of capillary	[mm]
n power-law index	[-]
\bar{n} screw speed	[rpm]
A activation energy	[J/mol]
G mass flow	[g/min]
P_3 pressure	[bar]
R gas constant	8.314 [J/mol K]
R_0 capillary radius	[mm]
T_0 reference temperature	400 [K]
θ mass temperature	[K]
ρ density	[g/cm ³]

Acknowledgement: The authors wish to thank to BorsodChem Zrt. Kazincbarcika for providing extrusionmeter for measurement and to the operator Gabriella Szemere for the precise and accurate measurement.

References:

- [1] R.B. Bird, R.C. Armstrong, O. Hassager, *Dynamics of Polymeric Liquids*, Vol. 1, Fluid Dynamics, Wiley, New York, 1987.
- [2] H. Schlichting, K. Gersten, *Boundary Layer Theory*, Springer-Verlag Berlin Heidelberg, 2000.
- [3] Bird, R.B. and H.C. Öttinger, Transport properties of polymeric liquids, *Ann. Revs. Phys. Chem.*, 54 (1992), 371-406.
- [4] Bird, R.B. and C.F. Curtiss, *Nonisothermal Polymeric Fluids*, *Rheol. Acta*, 35, 103-109, 1996.
- [5] Bird, R.B. and M.D. Graham, *General Equations of Newtonian Fluid Dynamics*, Chapter 3 of *The Handbook of Fluid Dynamics*, Richard W. Johnson, Editor, CRC Press, Boca Raton, 1998.
- [6] W.R. Schowalter, *Mechanics of Non-Newtonian fluids*, Pergamon Press, Oxford, 1978.
- [7] S. Middleman, *The Flow of High Polymers*, Interscience, New York, 1968.
- [8] B. Martin, Some analytical solutions for viscometric flows of power-law fluids with heat generation and temperature dependent viscosity, *Int. J. Nonlinear Mech.*, 2 (1967), 285-301.
- [9] H.L. Toor, The energy equation for viscous flow, *Industrial and engineering chemistry*, Vol. 48, No. 5, (1956), 922-926.
- [10] H.L. Toor, Heat transfer in forced convection with internal heat generation, *A.I.C.H.E. Journal*, Vol. 4, No. 3 (1958) 319-323.
- [11] R.E. Gee, J. B. Lyon, Nonisothermal flow of viscous non-newtonian fluids, *Industrial and engineering chemistry*, Vol. 49, No. 6, (1957), 956-960.
- [12] P.C. Sukaneck, Poiseuille flow of a power-law fluid with viscous heating, *Chemical Engineering Science*, 26 (1971), 1775-1776.
- [13] A. Lawal, D.M. Kalyon, Viscous Heating in Nonisothermal Die Flows of Viscoplastic Fluids With Wall Slip, *Chem. Eng. Science* 52 (1997), 1323-1337.
- [14] F. Rodriguez, *Principles of Polymer Systems*, 2nd ed., McGraw-Hill, 1987. p.536. ISBN0-07-Y66514-1
- [15] L. Macskási, A critical analysis of the models connecting molecular mass distribution and shear viscosity functions, *eXPRESS Polymer Letters*, 3(6) 2009, 385-399
- [16] <http://www.slovnaft.sk>